Phytochemistry 187 (2021) 112781

Contents lists available at ScienceDirect

Phytochemistry

journal homepage: www.elsevier.com/locate/phytochem

Screening of *in vitro* and *in silico* α-amylase, α-glucosidase, and lipase inhibitory activity of oxyprenylated natural compounds and semisynthetic derivatives

Immacolata Faraone [a,b], Daniela Russo [a,b], Salvatore Genovese [c], Luigi Milella [a,*], Magnus Monné [a], Francesco Epifano [c,**], Serena Fiorito [c]

[a] Department of Science, University of Basilicata, via dell'Ateneo Lucano 10, 85100, Potenza, Italy
[b] SpinoffBioActiPlant s.r.l., via dell'Ateneo Lucano 10, 85100, Potenza, Italy
[c] Department of Pharmacy, University Gabriele D'Annunzio of Chieti-Pescara, Via dei Vestini 31, 66100, Chieti Scalo, CH, Italy

ARTICLE INFO

Keywords:
Oxyprenylated natural compounds
Semisynthetic compounds
α-amylase inhibition
α-glucosidase inhibition
Pancreatic lipase inhibition
Molecular docking
Metabolic syndrome

ABSTRACT

Metabolic syndrome has several characteristic manifestations, including insulin resistance and dyslipidaemia, that demand therapeutic approaches, such as the inhibition of enzymes involved in nutrient absorption and digestion.This study aimed to evaluate the potential pharmacological use of natural compounds widespread in the plant kingdom and their semisynthetic compounds against target enzymes. Twenty-three oxyprenylated natural compoundswere investigated for their ability to inhibit α-amylase, α-glucosidase, and pancreatic lipase enzymes by *in vitro* assays. Moreover, *in silico* molecular docking was performed to analyse their binding capabilities into 3D structures. Farnesyloxyferulic acid, geranyloxyvanillic acid, nelumal A, and geranyloxyferulic acid showed the highest inhibition activity in all three *in vitro* enzyme assays. Moreover, *in silico* molecular docking of these four compounds was used to analyse their possible binding in 3D structures of the investigated enzymes. The results indicate that these compounds have considerable therapeutic potential for the treatment of metabolic syndrome, and further studies are warranted for their pharmacological development.

1. Introduction

Obesity has increased every year since 1980. At present, the number of overweight adults worldwide is about 1.9 billion, according to the World Health Organization, with the highest obesity rates in the following countries: United States, Mexico, New Zealand, and Hungary. Obesity, together with hypertension, hypertriglyceridemia, hyperglycemia, and hypoalphalipoproteinemia, are comorbidities present in metabolic syndrome (MetS) that increase morbidity and mortality, reducing the quality of life and resulting in a global public health care problem (Fernando et al., 2020). MetScan be influenced by both environmental and genetic factors. Insulin resistance, impaired glucose tolerance, and dyslipidemia are the main characteristic of the pathophysiology of MetS. MetSleadsto an increased risk of cardiovascular diseases, pancreatic and kidney dysfunction, non-alcoholic fatty liver disease, and cancer (liver, pancreas, breast, and bladder) (Baxter et al., 2006; Fernando et al., 2020; Wong et al., 2016). The chronic effects of MetS demand therapeutic intervention and, possibly, compounds able to reduce glucose and lipid blood levels with low side effects. One of the therapeutic strategies used in MetS is to interact with enzymes involved in nutrient digestion and absorption. In particular, the inhibition of enzymes involved in carbohydrate digestion, α-amylase, and α-glucosidase, is certainly important in postprandial hyperglycaemia control, typical of type 2 diabetes. In fact, the digestion of dietary starch is operated by α-amylase, releasing oligosaccharides that are further broken down by α-glucosidase to glucose, which is rapidly absorbed by the body (Awosika and Aluko, 2019). Moreover, hydrolysis of dietary lipids is catalysed by pancreatic lipase, and employing inhibitors of this enzyme is a strategy adopted in therapy for reducing both: fat absorption and weight (Spínola et al., 2020). The inhibitors of α-amylase and α-glucosidase, like acarbose, and inhibitors of lipase, like orlistat, are commonly used in clinical therapy to decrease hyperglycaemia and hyperlipidaemia as well as obesity (Buchholz and Melzig, 2016; Franco et al., 2020). Therefore, identifying compounds that are effective on all

* Corresponding author.
** Corresponding author.
E-mail addresses: luigi.milella@unibas.it (L. Milella), francesco.epifano@unich.it (F. Epifano).

https://doi.org/10.1016/j.phytochem.2021.112781
Received 11 December 2020; Received in revised form 10 April 2021; Accepted 11 April 2021
Available online 28 April 2021

these enzymes could reduce MetS related pathology, resulting in a more efficient drug therapy.

Since natural products are important sources of new drugs, our research aimed to investigate the inhibitory effects of 23 pure natural and semisynthetic compounds on the activity of α-amylase, α-glucosidase, and pancreatic lipase *in vitro,* aiming at identifying possible candidates for pharmacological therapy. Many of these compounds are natural oxyprenylated ferulic, umbelliferone derivatives and coumarins

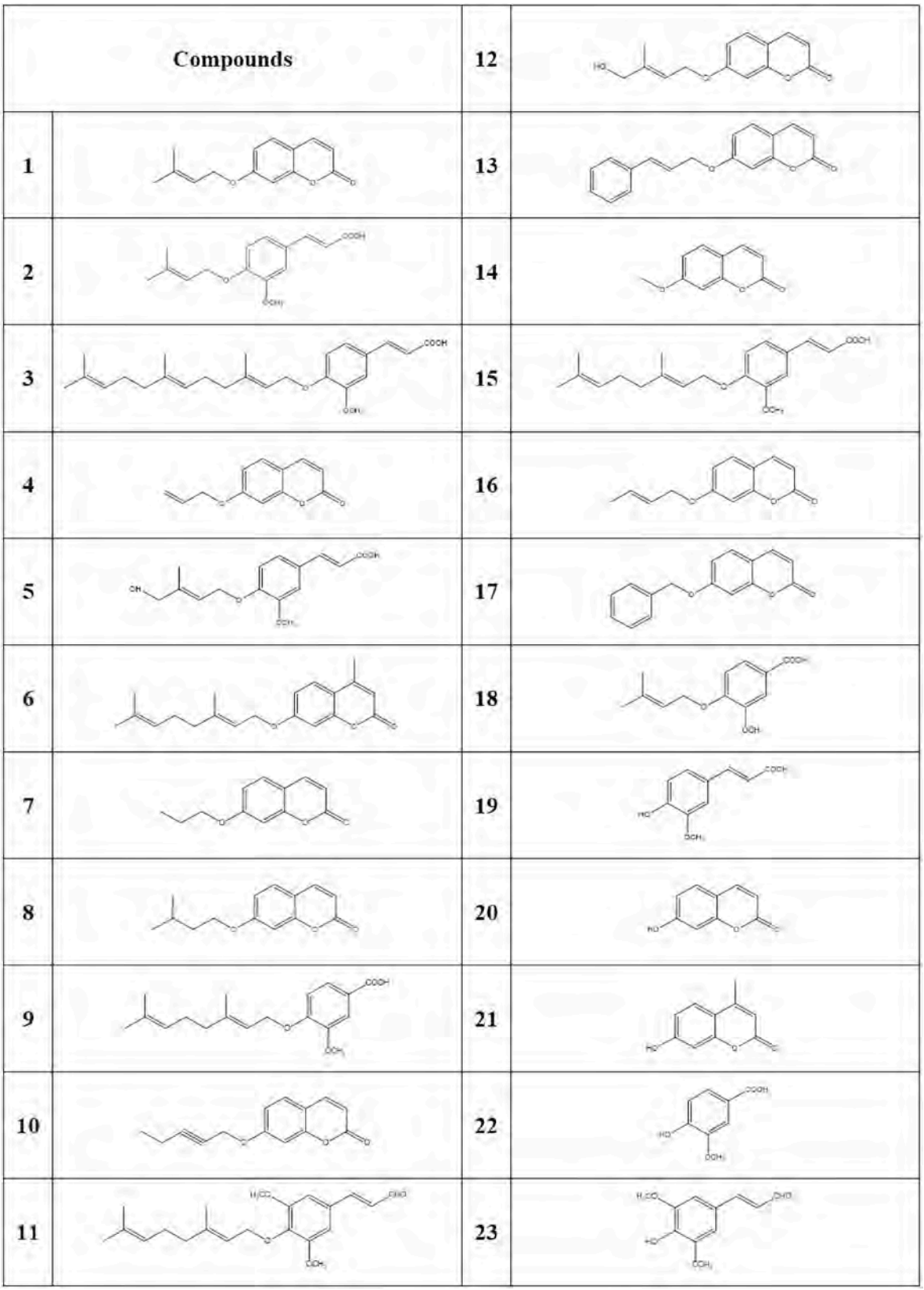

Fig. 1. Chemical structures of the 23 analysed pure natural and semisynthetic compounds.

that have been isolated from different plants, such as *Ferula foetida* L. (Apiaceae) or *Cinnamomum cassia* L. J.Presl (Lauraceae) The most efficient inhibitors of all three enzymes were selected for further analysis by docking them into structures of the three proteins *in silico* in an attempt to understand how the compounds may bind and exert their inhibitory activity. In fact, a combined *in vitro* and *in silico* approach is necessary to screen for active compounds to understand the possible molecular interactions affinity. Molecular docking is an important *in silico* technique normally used to predict the orientation between the receptor and the ligand (pure compound). This technique is employed in drug discovery because it is inexpensive and time-saving (Miners et al., 2004). For these reasons, the development of *in vitro* and *in silico* approaches is important to predict drug interactions, to possibly identify the pharmacophore, to reduce time and costs (FitzGerald et al., 2020).

2. Results and discussion

The 23 pure compounds (Fig. 1) were tested using three *in vitro* enzymatic assays to evaluate their α-amylase, α-glucosidase, and lipase inhibition ability. Among them, compounds **1–3**, **5**, **8**, **9**, **11**, **12**, **14**, and **18–23** are natural molecules (Gargaro et al., 2017), while the other molecules have semisynthetic origin (Table 1).

Acarbose, a commonly prescribed antidiabetic drug, was used as positive control in the α-amylase and α-glucosidase inhibition assays (Faraone et al., 2019), whereas orlistat, a drug currently used against fat absorption, was used as positive control in the lipase inhibition assay (Patil et al., 2017). The inhibitory activity of the analysed compounds increased proportionally with their concentration, indicating a clear dose-dependent effect. Compound **11**, nelumal A, an active principle isolated from a Chinese medicinal plant, *Ligularia nelumbifolia* (Bureau & Franch.) Hand.-Mazz (Compositae), showed the highest inhibitory activity against α-amylase with the same order of magnitude as that of acarbose (IC_{50} of 7.84 ± 0.58 μM and 5.56 ± 0.48 μM, respectively). The IC_{50} values of the pure compounds **3**, **5**, **9**, **12**, **15**, **17**, **18**, and **22**were comparable, and there was no statistical difference among them (Table 2 and Fig. 2 A). Moreover, it was not possible to determine IC_{50} for compounds **6**, **8**, **13**, and **20,** even when these compounds were tested at the highest concentration. To compare the inhibition activity of all tested substances, they were tested at the concentration of 31.25 μM, and in this set of experiments, compound **11** showed an inhibitory activity (99.75 ± 0.03%) that was higher than that of acarbose (75.75 ± 0.44%).

The activity of compounds tested against α-glucosidase is presented in Table 2. In this case, some compounds could not inhibit the enzyme

Table 1
Analysed pure natural and semisynthetic compounds. IUPAC name, trivial name (if any), and natural source.

Compound	IUPAC name	Trivial name	Origin	Reference
1	7-[(3-methyl-2-buten-1yl) oxy]-2H-1-benzopyran-2-one	7-isopentenyloxycoumarin	Rutaceae	Preziuso et al. (2020)
2	3-[3-Methoxy-4- [(3-methyl-2-buten1-yl) oxy] phenyl]-(2E)-propenoic acid	Boropinic acid	*Boronia pinnata* Sm. (Rutaceae)	Fiorito et al. (2019)
3	3-[3-Methoxy-4-[(2E,6E)-3,7,11-trimethyl-2,6,10-dodecatrien-1-yl]oxy]phenyl]-(2E)-propenoic acid	Farnesyloxyferulic acid	S.O.	Epifano et al. (2007)
4	7-(2-Propen-1-yloxy)-2H-1-benzopyran-2-one	7-allyloxyumbelliferone	S.O.	Gargaro et al. (2017)
5	3-[3-Methoxy-4-[(3-methyl-2-buten-4-ol-1-yl) oxy] phenyl]-(2E)-propenoic acid	no trivial name	*Boronia pinnata* Sm. (Rutaceae)	Di Giulio et al. (2016)
6	4-Methyl-7- [[(2E, 6E) −3, 7, 11-trimethyl-2, 6, 10-dodecatrien-1-yl] oxy] -2H-1-benzopyran-2-one	no trivial name	S.O.	Gargaro et al. (2017)
7	7-(2-Propyloxy)-2H-1-benzopyran-2-one	7-*n*propyloxyumbelliferone	S.O.	Gargaro et al. (2017)
8	7-(3-Methylbutoxy)-2H-1-benzopyran-2-one	7-dihydroisopentenyloxycoumarin	S.O.	Gargaro et al. (2017)
9	3-[3-Methoxy-4-[(3,7-dimethyl-octa-2,6-dienyl) oxy]-benzoic acid	4-geranyloxyvanillic acid	S.O.	Bruyère et al. (2011)
10	7-(2-Pentyn-1-yloxy)-2H-1-benzopyran-2-one	no trivial name	S.O.	Gargaro et al. (2017)
11	3-[4-[[(2E)-3,7-Dimethyl-2,6-octadien-1-yl]oxy]-3,5-dimethoxyphenyl]-(2E)-2-propenal	Nelumal A	*Ligularia nelumbifolia* (Bureau & Franchet) Handel-Mazzetti (Asteraceae)	Miyazaki et al. (2021)
12	7-(3-Methyl-2-buten-4-ol-1-yl)oxy-2H-1-benzopyran-2-onE	7-(3′-hydroxymethyl-3′-methylallyloxy) coumarin,	*Haplopappus multifolius* Phil ex Reiche (Rutaceae)	Fiorito et al. (2016)
13	7-[(3-Phenyl-2-propen-1-yl)oxy]-2H-1-benzopyran-2-one	7-styrylumbelliferone	S.O.	Gargaro et al. (2017)
14	7-Methoxy-2H-1-benzopyran-2-one	7-methoxyumbelliferone	Rutaceae	(Gargaro et al., 2017);
15	3-[4-[[(2E)-3,7-Dimethyl-2,6-octadien-1-yl]oxy]-3-methoxyphenyl]-(2E)-2-propenoic acid	4′-geranyloxyferulic acid	Rutaceae	Fiorito et al. (2019)
16	7-(2-buten-1-yl)oxy)-2H-1-benzopyran-2-one	no trivial name	S.O.	Gargaro et al. (2017)
17	7-Benzyloxy-2H-1-benzopyran-2-one	7-benzyloxyumbelliferone	S.O.	Gargaro et al. (2017)
18	3-Methoxy-4-[(3-methyl-2-buten-1-yl)oxy]-benzoic acid	isopentenyloxyvanillic acid	S.O.	Bruyère et al. (2011)
19	4-Hydroxy3-methoxyphenyl-(2E)-2-propenoic acid	ferulic acid	ubiquitous	Chaudhary et al. (2019)
20	7-Hydroxy-2H-1-benzopyran-2-one	umbelliferone	ubiquitous	da Cruz et al. (2020)
21	7-Hydroxy-4-methyl-2H-1-benzopyran-2-one	4-methylmbelliferone	S.O.	Nagy et al. (2015)
22	4-Hydroxy-3-methoxy-benzoic acid	vanillic acid,	ubiquitous	Brimson et al. (2019)
23	3-(4-Hydroxy-3,5-dimethoxyphenyl)- (2E)-2-propenal	sinapaldehyde	ubiquitous	Farah and Samuelsson (1992)

S.O. = semysinthetic origin.

Table 2
α-Amylase and α-glucosidase inhibitory activity of 23 pure natural and semi-synthetic compounds.

Compounds	α-Amylase inhibition assay		α-Glucosidase inhibition assay	
	% inhibition at 31.25 μM	IC_{50} μM	% inhibition at 400.00 μM	IC_{50} μM
Acarbose	75.75 ± 0.44^{a}	5.56 ± 0.48^{a}	43.94 ± 3.58^{a}	491.68 ± 37.22^{a,b}
1	13.49 ± 0.24 ^{b}	1410.89 ± 99.83 ^{b}	13.78 ± 0.65 ^{b}	nd
2	24.95 ± 0.15^{c}	1104.04 ± 41.93 ^{b,c}	Negative^{c}	nd
3	31.58 ± 0.27 ^{d}	160.87 ± 5.09^{a}	>100%^{d}	7.39 ± 0.35^{c}
4	24.92 ± 1.41^{c}	1892.59 ± 147.74 ^{d}	Negative^{c}	nd
5	53.31 ± 0.06^{e}	21.55 ± 0.82^{a}	30.70 ± 1.88^{e}	1031.81 ± 39.75 ^{d}
6	27.94 ± 1.48^{c}	nd	Negative^{c}	nd
7	21.47 ± 2.15^{f}	2827.15 ± 74.40^{e}	2.76 ± 0.26^{c}	1877.63 ± 32.36^{e}
8	18.03 ± 1.82 ^{g}	nd	34.56 ± 2.06^{e}	nd
9	46.47 ± 0.92 ^{h}	45.85 ± 3.84^{a}	51.68 ± 1.55^{f}	325.21 ± 11.41^{a,b,f}
10	16.11 ± 0.55 ^{b,g}	1036.06 ± 63.59^{c}	50.29 ± 3.32^{f}	381.51 ± 31.12^{a,b,f}
11	99.75 ± 0.03^{i}	7.84 ± 0.58^{a}	90.87 ± 1.93 ^{g}	145.39 ± 5.91^{c,f}
12	42.40 ± 0.35^{j}	69.19 ± 3.59^{a}	19.57 ± 0.27 ^{h}	1349.30 ± 83.63 ^{g}
13	15.07 ± 0.48 ^{b,g}	nd	Negative^{c}	nd
14	18.93 ± 0.63^{f,g}	1585.31 ± 117.15 ^{b,d}	47.54 ± 1.00^{a,f}	533.64 ± 36.00^{a,b,f}
15	45.38 ± 0.32 ^{h,j}	68.25 ± 1.87^{a}	60.11 ± 1.77^{i}	336.73 ± 22.96^{a,f}
16	26.90 ± 2.24^{c}	1006.19 ± 36.73^{c}	14.36 ± 0.82 ^{b}	nd
17	21.72 ± 0.35^{f}	343.04 ± 34.06^{a}	31.97 ± 1.33^{e}	666.51 ± 40.60 ^{b}
18	22.22 ± 0.60^{c,f}	204.25 ± 18.65^{a}	Negative^{c}	nd
19	19.72 ± 0.23^{f,g}	1102.02 ± 109.32 ^{b,c}	Negative^{c}	nd
20	20.05 ± 1.61^{f,g}	nd	8.12 ± 0.54^{j}	nd
21	19.13 ± 0.23^{f,g}	3618.73 ± 466.44^{f}	13.29 ± 0.60 ^{b}	2036.09 ± 4.86^{e,h}
22	31.61 ± 0.37 ^{d}	277.04 ± 20.07^{a}	10.09 ± 0.45 ^{b,j}	2156.04 ± 184.44 ^{h}
23	17.85 ± 0.67 ^{g}	3029.88 ± 32.43^{e}	16.75 ± 0.87 ^{b,h}	2202.38 ± 198.98 ^{h}

The enzymatic activity was shown as IC_{50} value (μM) and as %inhibition at a common final concentration. Results are expressed as the mean value of triplicate data ±standard deviation. Different superscripts in the same row (a-j) indicate significant difference ($p \leq 0.05$), 95% confidence limit, according to a one-way analysis of variance (ANOVA); nd = not determinable at tested concentrations.

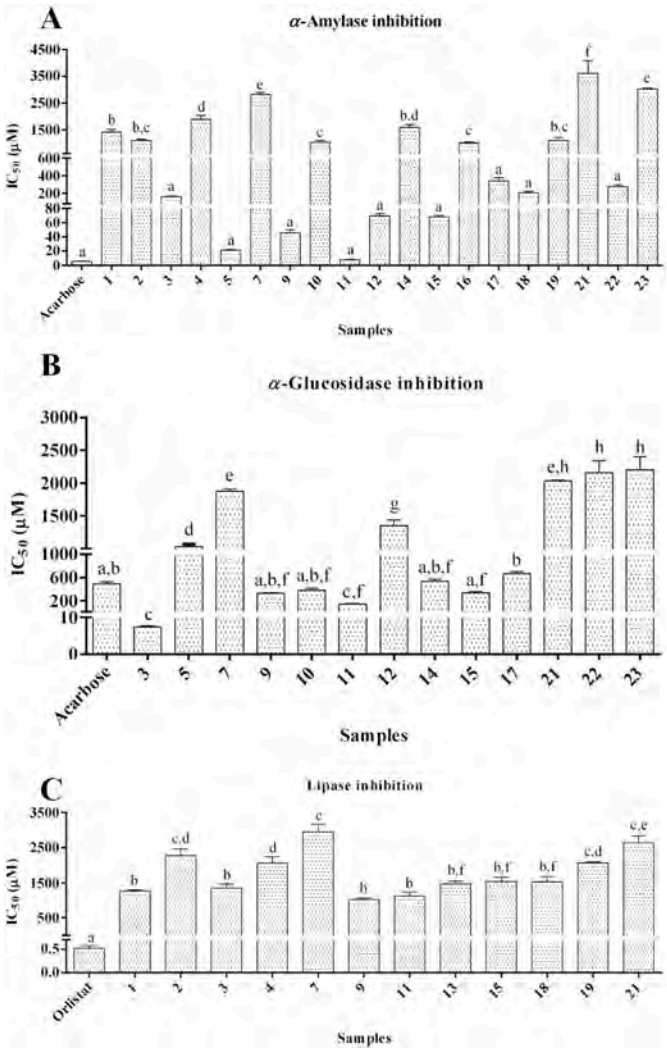

Fig. 2. *In vitro* inhibition activities.α-Amylase inhibition (A) andα-glucosidase inhibition (B) by acarbose and the pure active compounds. (C) Pancreatic lipase inhibition by orlistat and the pure active compounds. In each test, data are expressed as IC_{50} values in μM and values with the same letter (a–h) are not significantly different at $p \leq 0.05$ level, according to a one-way analysis of variance (ANOVA).

even when tested at the highest concentrations. However, compounds **3**, **9**, **10**, **11**, and **15** showed an interesting inhibitory activity, which was higher than acarbose (491.68 ± 37.22 μM). In particular, the activity of compound **3** is the highest, with an IC_{50} value of 7.39 ± 0.35 μM, almost two orders of magnitude more effective than that of the reference standard (Table 2 and Fig. 2 B).

Moreover, the inhibitory activity of the selected substances against pancreatic lipase was measured, and the results demonstrate that all compounds have a lower inhibitory effect than that of orlistat (0.52 ± 0.05 μM), which was used as the reference standard. Again, compounds **3**, **9**, and **11** were the most effective, together with compound **1** (Table 2 and Fig. 2 C).

In conclusion, the compounds that showed the highest inhibitory activity in all *in vitro* enzyme assays were compounds **3**, **9**, and **11**, followed by compound **15**. The four substances have a 4′-geranyloxy-3′-methoxyphenyl unit in common, where each compound presents various 1′ substituents (carboxylic acid (**9**), trans-propenoic acid (**3** and **15**) or trans-propenal (**11**)) and in one case a 5′-methoxy (**11**) and in another a farnesyl instead of a geranyl unit (**3**). Thus, interestingly, concerning all the other tested compounds, **9**, **11**, and **15** have in common the side chain constituted by geranyl unit, whereas compound **3** has a farnesyl unit (a geranyl elongated with one more isoprene unit). Among all tested compounds, only one more compound has the geranyl group, the 7-geranyloxy-4-methylcoumarin (compound **6**). However, this compound did not show activity at the tested concentrations in the three tests carried out. Starting from this observation, it might be hypothesised that the presence of a CHas an additional moiety negatively interferes with the inhibitory properties of the target enzymes. Perhaps, the inactivity of compound **6** could be due to the methylcoumarin structure, which completes the molecule; in fact, also the compound **21**, the 7-hydroxy-4-methylcoumarin, with the same structure, showed a low inhibitory activity in all assays. Compound **9**, a prenyloxyphenylpropanoid vanillic acid derivative, was previously tested for its *in vivo* neuroprotective activity using the mouse maximal electroshock-induced seizure model (Genovese et al., 2009)and for its inhibitory effects on nitric oxide production in bacterial

lipopolysaccharide (LPS)-stimulated with a low activity ($IC_{50} > 200$ μM) (Genovese et al., 2013). Moreover, nelumalA (compound **11**) is effective against aromatase, a member of the cytochrome P450 family, with a potency comparable to anastrozole, a known aromatase inhibitor. These results have been previously demonstrated on two human cell lines, human embryonic kidney 293T cells (HEK293T) and human granulosa-like tumour cells (Epifano et al., 2014). In addition, the *in vitro* growth-inhibitory activity of this oxyprenylated natural phenylpropanoid was tested on six human cancer cell lines using MTT colourimetric assays (Bruyère et al., 2011). Aromatase, together with the three enzymes investigated in the present work, are involved in risk for some cancers and the progression of MetS (Chen et al., 2015; Hargrove et al., 2011; Subbaramaiah et al., 2011).For these reasons, the action carried out by nelumal A could represent a valid therapeutic strategy in patients with MetS. The 4′-geranyloxyferulic acid (GOFA), compound **15**, was also known as a natural colon cancer chemopreventive agent (Genovese et al., 2010). Moreover, the 3-(4′-farnesyloxy-3′-methoxyphenyl)-2-trans propenoic acid (compound **3**) was previously evaluated for its *in vitro* inhibition ability against farnesyl transferase (FTase) and geranylgeranyltransferase I (GGTase I). The sample did not show activity on FTase, while it inhibited GGTase I with 83.90% inhibition and an IC_{50} value of 66 μM (Epifano et al., 2007).

It is interesting to underline that, as previously reported in the literature, the addition of isoprenoid chains to natural compounds can increase the pharmacological potential of the native non-prenylated products (Genovese et al., 2018).

Molecular docking was performed to analyse the binding capabilities of compounds **3**, **9**, **11**, and **15**into 3D-structures of human pancreatic α-amylase, intestinal α-glucosidase, and pancreatic lipase enzymes because they were shown the most potent inhibitors considering the measured IC_{50} values (Fig. 2 and Tables 2 and 3). The structures used in the docking study were human proteins in inhibitor-bound conformations: α-amylase, which has 97% sequence identity to the salivary form of the enzyme and 87% identity to the porcine counterpart used in the assay (the latter two sharing 86% identity); α-glucosidase, which, although low sequence similarity to the yeast protein used in the inhibition assay, belongs to the same protein superfamily and have the same catalytic triad; and lipase, for which the species origin of the assay enzyme is unknown.In the docking procedure, the side chains of the residues of the active site pocket and the tested ligand compounds are given conformational freedom and solutions with the lowest binding energies (highest affinities) are calculated upon searches in the so-called conformational space.

Table 3
Pancreatic lipase inhibitory activity of 23 pure natural and semisynthetic compounds.

Samples	% inhibition at 400.00 μM	IC_{50} (μM)
Orlistat	100%[a]	0.52 ± 0.05[a]
1	44.75 ± 0.31 [b]	1263.28 ± 27.20 [b]
2	25.08 ± 0.88[c]	2273.73 ± 186.14[c,d]
3	23.89 ± 1.06[c,d]	1342.02 ± 116.15 [b]
4	23.99 ± 1.10[c,d]	2055.98 ± 181.56 [d]
5	21.02 ± 1.32 [d]	nd
6	14.93 ± 0.66[e]	nd
7	31.48 ± 1.10[f]	2945.77 ± 215.06[e]
8	27.42 ± 0.66[c]	nd
9	44.90 ± 0.22 [b]	1024.13 ± 36.01 [b]
10	14.15 ± 0.88[e]	nd
11	42.87 ± 0.88 [b,g]	1116.67 ± 109.79 [b]
12	23.93 ± 1.18 [d]	nd
13	40.58 ± 0.18 [g,h]	1464.32 ± 85.14 [b,f]
14	7.60 ± 0.44[i]	nd
15	35.85 ± 1.99[j]	1530.09 ± 125.59 [b,f]
16	20.81 ± 1.41 [d]	nd
17	38.29 ± 1.98 [h,j]	nd
18	36.63 ± 0.88[j]	1522.17 ± 144.97 [b,f]
19	23.52 ± 1.77 [d]	2070.48 ± 28.34[c,d]
20	12.90 ± 0.88[e,k]	nd
21	22.89 ± 0.88 [d]	2628.18 ± 202.76[c,e]
22	16.96 ± 0.88[e]	nd
23	13.37 ± 0.66[e,k]	nd

The enzymatic activity was shown as IC_{50} value (μM) and as %inhibition at a common final concentration. Results are expressed as the mean value of triplicate data ±standard deviation. Different superscripts in the same row (a-k) indicate significant difference ($p \leq 0.05$), 95% confidence limit, according to a one-way analysis of variance (ANOVA); nd = not determinable at tested concentrations.

The highest-ranking docking results of compounds **3**, **9**, **11**, and **15** inα-amylase were analysed and compared to each other and the binding of acarbose (Fig. 3). The docked compounds interact with various residues in the substrate-binding pocket, of which many overlaps, but only two (E248 and I250) bind to all four of them (Fig. 3 A-E). The binding residues also include two of the residues indispensable for catalysis (D212 and E248). Most of the interactions between the ligand and the protein are hydrophobic, and very few hydrogen bonds are found, which is not surprising given the mainly hydrophobic nature of the compounds and the very few potential hydrogen bond donors and acceptors. The carboxylic groups (of the 1′-phenyl substituent transpropenoic acid) of compound **3**and **15**, which only differ from each other in having a farnesyl or geranyl moiety in the 4′ position of the phenyl ring, both form hydrogen bonds with E255 and have superimposed positions (Fig. 3 A, D, **and E),** and the aldehyde of **11** (also in the 1′ phenyl substituent transpropenal) also stretches towards this residue (Fig. 3 C and E). It is noteworthy that all four compounds bind in a similar orientation in α-amylase with the position of their aromatic rings almost superimposed, and in the case of compounds **3** and **15** totally (Fig. 3 E), whereas the farnesyl/geranyl tails (4′-phenyl substituents) are positioned more variably. The more different position of compound **9** may be explained by it havingonly a carboxylate group as 1′-phenyl substituent and therefore not reaching E255 (too short), but it makes a hydrogen bond to E248 and probably, as a consequence, its aromatic ring is positioned more differently from those of compounds **3**, **11**, and **15** (Fig. 3 B and E). The binding energies for the four compounds in α-amylase calculated by AutodockVinarange from −7.7 to −9.3 kcal/mol and are compatible with high affinities. The docking results of the four compounds in α-amylase were compared to the position of the inhibitor acarbose, which was present in the original enzyme structure (Fig. 3 F), because some of the dimensions of the hexose-analogue chain resemble those of the compounds, although it is chemically very different from the tested substances due to its high hydrophilicity and make very different interactions with the protein. The 1′-phenyl substituents of compound **3, 11**, and **15** cover the position corresponding to the first hexose of acarbose, the aromatic rings approximately of all four compounds are positioned on the second hexose of acarbose and their farnesyl/geranyl tails cover the third hexose, which covers the active site residues (Fig. 3 A-E). Therefore, given the structural similarity between compounds **3**, **9**, **11**, and **15** and the resemblance in conformation, orientation, position, and contact-making, in which they bind to α-amylase, it is likely that they bind the enzyme with high affinity in a similar way and that they inhibit the entrance of the substrate (or accessibility of the active site residues) in analogy to acarbose.

Compounds **3**, **9**, **11**, and **15** were also docked into the structure of α-glucosidase, analysed and compared to each other and the binding of acarbose, which was present in the original structure of this enzyme too (Fig. 4). All four compounds interact with several of the residues of the narrower and deeper binding pocket of α-glucosidase (compared to that of α-amylase), and among the residues participating in ligand binding are the active site residues D1420 and D1526 (Fig. 4 A-E). The latter residue, together with W1369 and F1560, are bound by all four compounds; however, many of the other binding resides are also in common for more than one compound. The 1′-phenyl substituents are penetrating the deepest part of the cleft, and the carboxylic groups of compounds **3**, **9**, and **15**form different hydrogen bonds, the latter two with the active site residue D1420 (Fig. 4 A, B and D). The positions of aromatic rings of

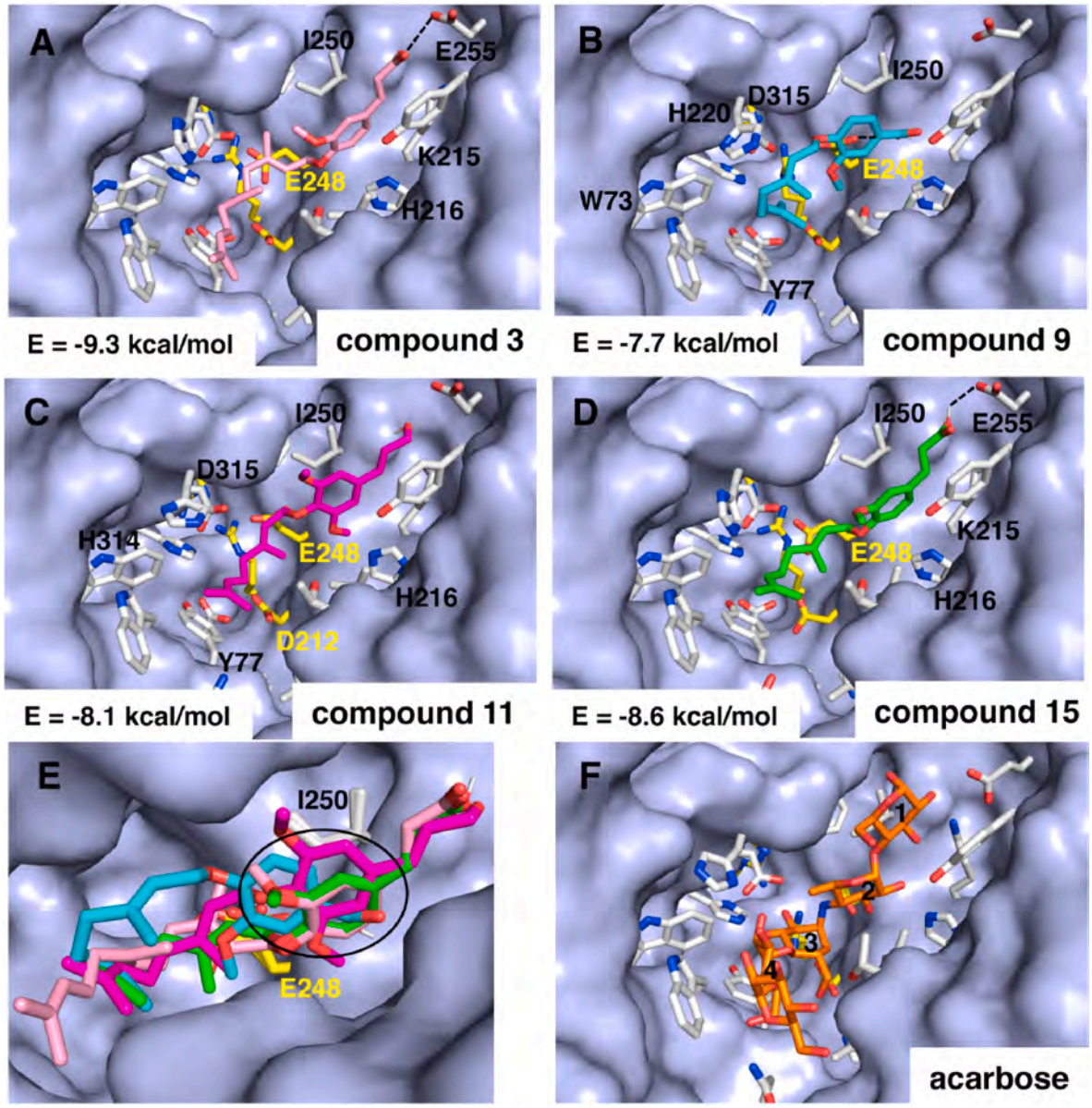

Fig. 3. Docking of compounds 3, 9, 11, and 15 in human α-amylase and α-glucosidase enzymes. The original structures of α-amylase (1XD0) and α-glucosidase (3TOP) enzymes contain the inhibitor acarbose (carbons coloured in orange and hexoses numbered in A and F, respectively). The docking results in α-amylase (B-E, light grey surface) and α-glucosidase (G-J, beige) enzymes with compounds 3 (pink, B and G), 9 (cyan, C and H), 11 (magenta, D and I), and 15 (green, E and J) are shown with their respective binding energies. The carbons of the residues lining the binding pocket are coloured in white, with the active site residues in yellow (R210, D212, E248, and R352 in α-amylase; D1420, E1423, and D1526 in α-glucosidase enzyme). Residues making hydrogen bonds with the ligands are indicated (B-E and G-J). (For interpretation of the references to colour in this figure legend, the reader is referred to the Web version of this article.)

compounds **3**, **11**, and **15** almost overlap, probably due to a similar length 1′-phenyl substituent, whereas that of **9** penetrates further into the pocket with its shorter 1′-carboxylate (Fig. 4 E). Regarding their aromatic rings, the farnesyl/geranyl tails of all four compounds linger back towards the entrance of the binding pocket with somewhat different conformations (Fig. 4 E). However, taken together, all four compounds bind to α-glucosidase in a quite similar orientation. The calculated binding energies of the docking of compounds **3**, **9**, **11**, and **15** in α-glucosidase, ranging from −8.1 to −8.7 kcal/mol, correspond to quite considerable affinity. In comparison, acarbose penetrates with hexose one and two deep into the narrow binding pocket covering the active site residues, whereas the other hexoses are towards the binding pocket entrance (Fig. 4 F). In the docking results, the aromatic rings of compounds **3**, **11**, and **15** are positioned corresponding to the second hexose of acarbose and the propenoic carboxylate/aldehyde moiety (1′-phenyl substituent) to the first hexose (Fig. 4 A, C, D, **and F**), whereas compound **9**, which lacks this moiety, has the aromatic ring approximately where the first hexose is found (Fig. 4 B and F). Thus, it is probable that compounds **3**, **9**, **11**, and **15** that have structural similarities bind α-glucosidase in a similar way and block the substrate from interacting with the catalytic residues by tight binding in the active site, which is like the inhibition mechanism of acarbose in this enzyme and the conclusions of the docking results with α-amylase.

The docking results of the four compounds into lipase were analysed in the same way as those of α-amylase and α-glucosidase. The substrate-binding site of lipase is a long cleft closed on one side, with the catalytic residues in the centre. In the docking results, compounds **3**, **9**, **11**, and **15** are positioned with the hydrophobic farnesyl/geranyl moiety above the catalytic residues and towards the open part of the binding cleft, whereas the aromatic rings are on the other half of the cleft and 1′-

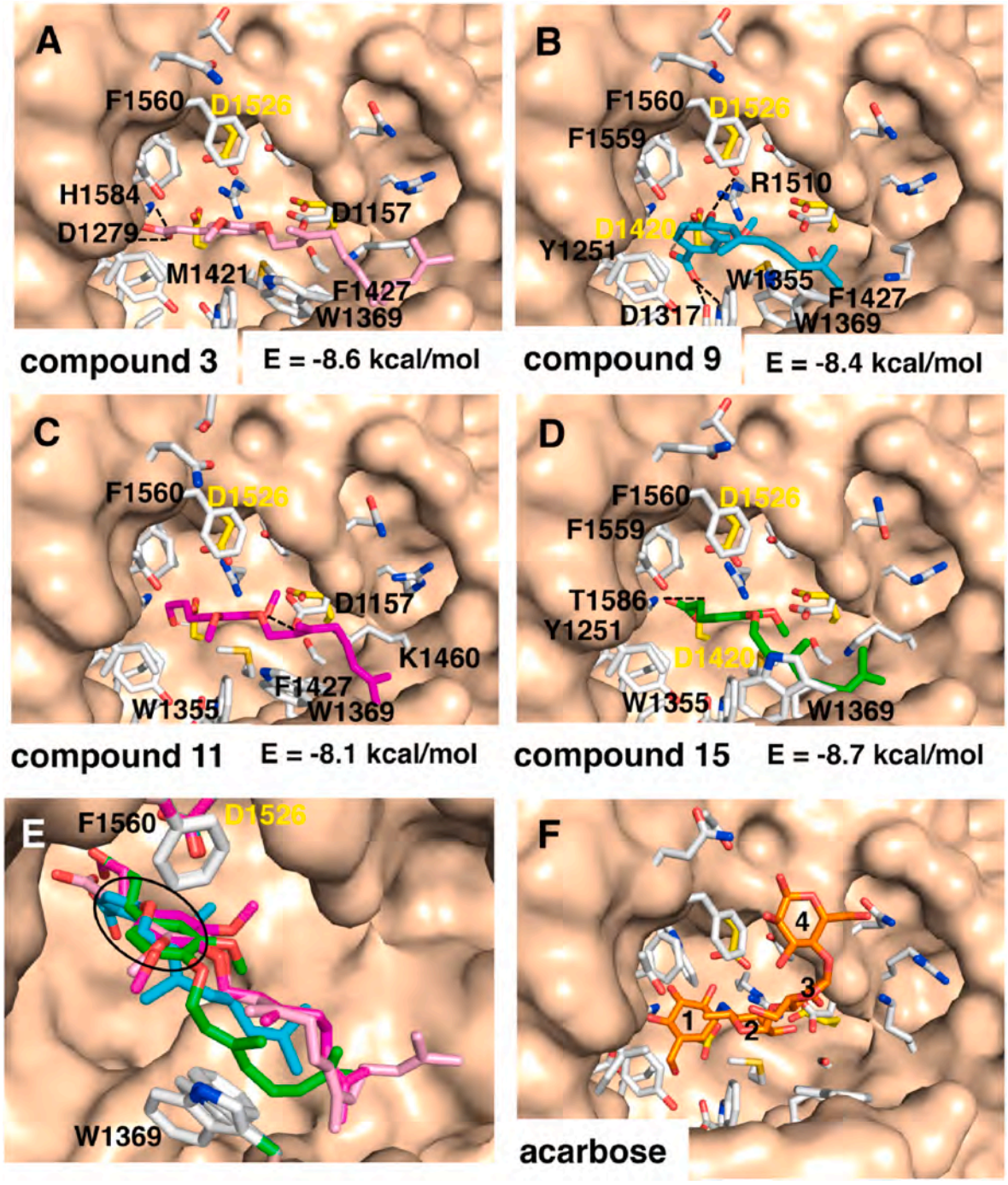

Fig. 4. Docking of compounds 3, 9, 11, and 15 in human lipase enzyme. The original structure of the lipase enzyme (1LPB) contains the inhibitor methoxyundecylphosphinic acid (MUP, carbons coloured purple (A)). The docking results in lipase enzyme (B-E, green surface) with compounds 3 (pink, B), 9 (cyan, C), 11 (magenta, D), and 15 (green, E) are shown with their respective binding energies. The carbons of the residues lining the binding pocket are coloured in white, with the active site residues in yellow (S169, D193, and H280). Residues making hydrogen bonds with the ligands are indicated (B–E). (For interpretation of the references to colour in this figure legend, the reader is referred to the Web version of this article.)

phenyl substituents are interacting, with hydrogen bondsfor compounds **3**, **9**, and **15**, with the residues closing the cleft (Fig. 5 A-D).In this case, many of the binding residues are in common between the compounds but are highly variable, and only F94, D96, H168, and H280 overlap for all four compounds (Fig. 5 E). H280 and S169, which are part of the catalytic triad, often participate in binding. Although the 1′-phenyl substituents of compounds **3** and **11** are different, they are quite well superimposed, including with their aromatic rings (Fig. 5 E), whereas these entities of **9** and **15** are located differently, which is interesting since the 1′-phenyl substituent of **15** is identical to that of **3**. In contrast, it seems that the farnesyl/geranyl tails are quite well superimposed, maybe with the exception **9**, towards the open part of the cleft after the restriction between F94 and the catalytic residue H280 (Fig. 5 E), which might suggest that these parts of the molecules are binding similarly and more specifically. The binding energies in the highest-ranking docking solutions of the four compounds in lipase range from −9.6 to −10.3 kcal/mol, which suggest elevated potential of high-affinity binding of the ligands. Compared to the binding of methoxyundecylphosphinic

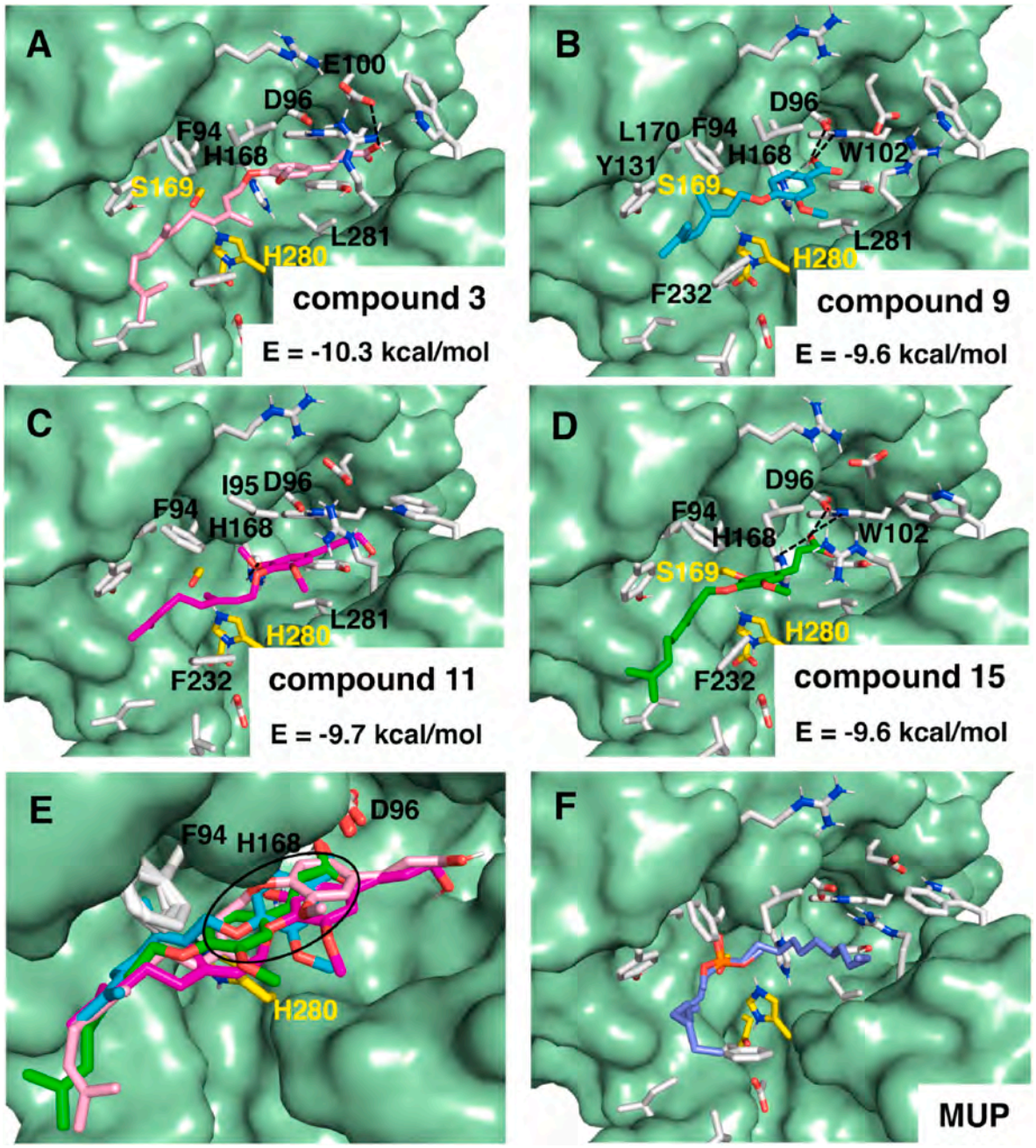

Fig. 5. Docking of compounds 3, 9, 11 and 15 in human lipase. The structure of lipase (green surface) with the residues lining the binding pocket (sticks with white carbons) and the catalytic resides (S169, D193 and H280 in yellow). The docking results in lipase with compounds 3 (pink, A), 9 (cyan, B), 11 (magenta, C) and 15 (green, D) are shown with their main interacting residues labelled, hydrogen bonds and binding energies. (E) Zoom in on the superimposition of the docked compounds 3, 9, 11 and 15 (coloured as in A-D) with the position of the aromatic rings encircled and the residues, which interact with all compounds of them, are labelled. (F) The original structure of lipase (1LPB) contains the inhibitor methoxy-undecylphosphinic acid (MUP in purple). (For interpretation of the references to colour in this figure legend, the reader is referred to the Web version of this article.)

acid (MUP), which was present in the original structure of lipase (Fig. 5 F), the compounds **3**, **9**, **11**, and **15**are positioned with the hydrophobic geranyl moiety in correspondence to one of the acyl chains of MUP, which has the phosphinic group in proximity to the catalytic triad. Whereas the aromatic rings and the phenyl and 1′-phenyl substituents of the compounds penetrate towards the closed part of the cleft, the other acyl chain of MUP exits the pocket (Fig. 5 A-D and F). In conclusion, the docking results for lipase also suggest that all four compounds bind the protein in a similar orientation and with similar interactions, mimicking the action of MUP; however, the farnesyl/geranyl tails (4′-phenyl substituents) interact more specifically probably in the part of the binding cleft where the hydrophobic parts of the fatty acids bind. Meanwhile, the phenyls (and 1′-phenyl substituents) bind more differently in correspondence to where the glycerol moiety of the natural substrate most likely binds.

The general conclusion of the docking results of compounds **3**, **9**, **11**, and **15** interactions with α-amylase, α-glucosidase, and pancreatic lipase, while keeping the enzyme inhibition experiments in mind, is that all three enzymes probably require both aromatic 3′-methoxyphenyl ring with variable 1′-substituents on the one hand and a 4′-polyisoprene of at least the length of a geranyl chain on the other hand to make the necessary number of interactions for tight binding and inhibition.

Our work encourages the need for further research on these molecules. Here, we have demonstrated that some of them exert an important inhibitory activity against α-amylase, α-glucosidase, and lipase enzymes.

3. Conclusion

Among the tested compounds, **3**, **9**, **11**, and **15** were the most promising. Above all, these four pure compounds are candidates and possible drugs to be used in patients with MetS, given their ability to inhibit enzymes involved in postprandial hyperglycemia and lipid metabolism. These results suggest that the compounds have significant pharmacological potential that needs further investigation to confirm and clearly understand the complete mechanistic aspects related to their activity and toxicological effects.

4. Experimental

4.1. Chemicals

Reagents and standards as 4-*p*-nitrophenyl-α-D-glucopyranoside, α-glucosidase from *Saccharomyces cerevisiae* (CAS number: 9001-42-7), α-amylase from hog pancreas (CAS number: 9000-90-2), dimethyl sulfoxide (DMSO), iodine, potassium iodide, potassium phosphate monobasic, sodium carbonate, sodium chloride, starch, acarbose and orlistat were purchased from Sigma-Aldrich (Milan, Italy). The QuantiChrom™ lipase assay kit was purchased from BioAssay Systems (BioAssay Systems, Hayward, CA, USA).

4.2. Preparation of samples

Investigated samples have been synthesized following the same general procedure as already reported (yields > 81.40%). Their purity was assayed by HPLC and resulted to be >98%. ^{1}H and ^{13}C NMR data were in full agreement with those previously reported for the same compounds (Bruyère et al., 2011; Gargaro et al., 2017).Different concentrations of 23 pure compounds (25000.00–0.03 μM) were prepared with pure dimethyl sulfoxide (DMSO) (Kayukova et al., 2019) and tested for their *in vitro* enzymatic activity.

4.3. Potential antidiabetic activity

4.3.1. α-Amylase inhibition

The ability of samples to inhibit the α-amylase enzyme was determined using starch as substrate, by the Caraway-Somogyi iodine/potassium iodide method with slight modifications (Herrera et al., 2019; Zengin et al., 2016).α-Amylase enzyme solution (50 μL, 5 U/mL) was added to 25 μL of different concentrations of each sample and incubated at 37 °C for 10 min. After this pre-incubation, 100 μL of 1% starch solution were added and the reaction was incubated for another 10 min at 37 °C. Then, the reaction was stopped adding 25 μL of HCl 0.1 N. In order to measure the absorbance of samples, in each well of plate was added the dye, iodine–potassium iodide solution (KI/I_2 1:5, 50 μL); the absorbance was read at 630 nm while the plate was incubated at 37 °C for 12 min; data were reported after 10'. The blank of each concentration was prepared by adding all reaction reagents without α-amylase enzyme solution. Solvent alone and solvent with acarbose were used instead samples in the negative and positive controls, respectively, following the same procedure used for tested samples.

4.3.2. α-Glucosidase inhibition

The ability of samples to inhibit α-glucosidase enzyme was evaluated using a previously described method, with slight modifications (Braca et al., 2018; Faraone et al., 2020). Different concentrations of each sample (20 μL) were added to 50 μL of buffer and 40 μL of enzyme (0.1 U/mL). The reaction mix was pre-incubated at 37 °C for 10′ and then 40 μL of the substrate 4-*p*-nitrophenyl-α-D-glucopyranoside (2.5 mM) were added. The plate was again incubated for 15 min at 37 °C; after that, 100 μL of sodium carbonate 0.2 M were added and the absorbance was immediately monitored at 405 nm. Acarbose and DMSO were used as positive and negative controls, respectively.

4.4. Pancreatic lipase inhibition

Pancreatic lipase activity was measured using a QuantiChrom lipase assay kit (DLPS-100; BioAssay Systems, Hayward, CA, USA) according to manufacturer's instructions at 37 °C, with slight modifications (Hasan et al., 2009; QuantiChromTM Lipase Assay). In this colorimetric assay, also known as BALB method, the cleavage of dimercaptopropanol-tributyrate (BALB) operated from lipase gives SH groups that react with 5,5′-dithiobis (2-nitrobenzoic acid) (DTNB) allowing to get a yellow coloured product directly proportional to the enzymatic activity of the sample and monitored at 412 nm. DMSO and orlistat were used as negative and positive controls of the reaction, respectively (Patil et al., 2017).

4.5. In silico molecular docking

Molecular docking was performed by AutoDockVina (Trott and Olson, 2010) with conformationally flexible compounds **3**, **9**, **11** and **15** into the human protein structures of pancreatic α-amylase enzyme (PDB ID: 1XD0) (Li et al., 2005), small intestine α-glucosidase enzyme (PDB ID: 3TOP) (Ren et al., 2011) and pancreatic lipase enzyme (PDB ID: 1LPB) (Egloff et al., 1995). The side chains of the residues in the substrate binding pocket of each protein were chosen to have conformational flexibility during the docking: α-amylase enzyme (W58, W59, Y62, Q63, D96, V98, H101, Y151, L162, T163, L165, R195, D197, K200, H201, D233, I235, E240, F256, N298, H299, D300, H305 and R337), α-glucosidase enzyme (K1156, D1157, Q1158, P1159, Y1167, Y1251, D1279, I1280, Q1286, I1315, D1317, W1355, W1369, Q1372, K1377, W1418, D1420, M1421, E1423, S1425, F1427, K1460, R1510, W1523, D1526, T1528, D1555, F1559, F1560, Q1561, R1582, H1584, T1586 and I1587) and lipase enzyme (F77, I78, D79, E83, W85, R111, Y114, H151, S152, L153, D176, P180, D205, I209, L213, F215, W252, R256, H263, L264 and Y267).The docking results were analysed by PyMOL and PISA (Krissinel and Henrick, 2007).

4.6. Instruments and statistical analysis

All spectrophotometric measurements were done in 96-well microplates on a UV/vis spectrophotometer SPECTROstar^{Nano} (BMG Labtech, Ortenberg, Germany). Each assay was performed in triple triplicate and the data were expressed as mean of the concentration (in μM) of the sample required to inhibit the activity of the enzyme by 50% (IC_{50}) calculated by non-linear regression analysis ±standard deviation; where it was not possible to reach IC_{50}, data were also shown as percentage inhibition at a final common concentration in each test. The correlation among used assays was verified by the calculation of *p* value by one-way analysis of variance (ANOVA) using GraphPad Prism 5 Software (San Diego, CA, USA). Only the $p \leq 0.05$ was considered significant.

Funding

This research did not receive any specific grant from funding agencies in the public, commercial, or not-for-profit sectors.

Declaration of competing interest

The authors declare that they have no known competing financial interests or personal relationships that could have appeared to influence the work reported in this paper.

Acknowledgements

The authors are greatly thankful for financial support to the Italian Ministry of the Economic Development "Fondo per la Crescita Sostenibile—Sportello Agrifood" PON "I&C" 2014-2020, Prog n. F/200099/03/X45—CUP: B31B19000590008 COR: 1853255 and to Regional Project "ALIMINTEGRA, GO NUTRIBAS" financed on 16.1 PSR Basilicata founding ex D.G.R. n° 312/17 CUP: C31G18000210002.

References

Awosika, T.O., Aluko, R.E., 2019. Inhibition of the in vitro activities of α-amylase, α-glucosidase and pancreatic lipase by yellow field pea (Pisum sativum L.) protein hydrolysates. Int. J. Food Sci. Technol. 54, 2021–2034. https://doi.org/10.1111/ijfs.14087.

Baxter, A.J., Coyne, T., McClintock, C., 2006. Dietary patterns and metabolic syndrome-a review of epidemiologic evidence. Asia Pac. J. Clin. Nutr. 15, 134–142.

Braca, A., Sinisgalli, C., De Leo, M., Muscatello, B., Cioni, P.L., Milella, L., Ostuni, A., Giani, S., Sanogo, R., 2018. Phytochemical profile, antioxidant and antidiabetic activities of Adansonia digitata L. (Baobab) from Mali, as a source of health-promoting compounds. Molecules 23, 3104. https://doi.org/10.3390/molecules23123104.

Brimson, J.M., Onlamoon, N., Tencomnao, T., Thitilertdecha, P., 2019. Clerodendrum petasites S. Moore: the therapeutic potential of phytochemicals, hispidulin, vanillic acid, verbascoside, and apigenin. Biomed. Pharmacother. 118 https://doi.org/10.1016/j.biopha.2019.109319.

Bruyère, C., Genovese, S., Lallemand, B., Ionescu-Motatu, A., Curini, M., Kiss, R., Epifano, F., 2011. Growth inhibitory activities of oxyprenylated and non-prenylated naturally occurring phenylpropanoids in cancer cell lines. Bioorg. Med. Chem. Lett 21, 4174–4179. https://doi.org/10.1016/j.bmcl.2011.05.089.

Buchholz, T., Melzig, M.F., 2016. Medicinal plants traditionally used for treatment of obesity and diabetes mellitus–screening for pancreatic lipase and α-amylase inhibition. Phytother Res. 30, 260–266. https://doi.org/10.1002/ptr.5525.

Chaudhary, A., Jaswal, V.S., Choudhary, S., Sonika, Sharma A., Beniwal, V., Tuli, H.S., Sharma, S., 2019. Ferulic acid: a promising therapeutic phytochemical and recent patents advances. Recent Patents Infla 13, 115–123. https://doi.org/10.2174/1872213x13666190621125048.

Chen, J., Shen, S., Tan, Y., Xia, D., Xia, Y., Cao, Y., Wang, W., Wu, X., Wang, H., Yi, L., 2015. The correlation of aromatase activity and obesity in women with or without polycystic ovary syndrome. J. Ovarian Res. 8, 11. https://doi.org/10.1186/s13048-015-0139-1.

da Cruz, L.F., de Figueiredo, G.F., Pedro, L.P., Amorin, Y.M., Andrade, J.T., Passos, T.F., Rodrigues, F.F., Souza, I.L.A., Goncalves, T.P.R., Lima, L.A.R.D., Ferreira, J.M.S., Araujo, M.G.D., 2020. Umbelliferone (7-hydroxycoumarin): a non-toxic antidiarrheal and antiulcerogenic coumarin. Biomed. Pharmacother. 129, 130. https://doi.org/10.1016/j.biopha.2020.110843, 110432, 2020.

Di Giulio, M., Genovese, S., Fiorito, S., Epifano, F., Nostro, A., Cellini, L., 2016. Antimicrobial evaluation of selected naturally occurring oxyprenylated secondary metabolites. Nat. Prod. Res. 30, 1870–1874. https://doi.org/10.1080/14786419.2015.1079908.

Egloff, M.-P., Marguet, F., Buono, G., Verger, R., Cambillau, C., van Tilbeurgh, H., 1995. The 2.46. ANG. resolution structure of the pancreatic lipase-colipase complex inhibited by a C11 alkyl phosphonate. Biochemistry 34, 2751–2762.

Epifano, F., Curini, M., Genovese, S., Blaskovich, M., Hamilton, A., Sebti, S.M., 2007. Prenyloxyphenylpropanoids as novel lead compounds for the selective inhibition of geranylgeranyl transferase I. Bioorg. Med. Chem. Lett 17, 2639–2642. https://doi.org/10.1016/j.bmcl.2007.01.097.

Epifano, F., Genovese, S., Fiorito, S., Nde, C.M., Clyne, C., 2014. Nelumal A, the active principle of Ligularia nelumbifolia, is a novel aromatase inhibitor. Nat Prod Commun 9, 823–824.

Farah, M.H., Samuelsson, G., 1992. Pharmacologically active phenylpropanoids from senra-incana. Planta Med. 58, 14–18. https://doi.org/10.1055/s-2006-961380.

Faraone, I., Rai, D.K., Russo, D., Chiummiento, L., Fernandez, E., Choudhary, A., Milella, L., 2019. Antioxidant, antidiabetic, and anticholinesterase activities and phytochemical profile of Azorella glabra Wedd. Plants 8, 265. https://doi.org/10.3390/plants8080265.

Faraone, I., Russo, D., Chiummiento, L., Fernandez, E., Choudhary, A., Monné, M., Milella, L., Rai, D.K., 2020. Phytochemicals of Minthostachys diffusa Epling and their health-promoting bioactivities. Foods 9, 144. https://doi.org/10.3390/foods9020144.

Fernando, I.S., Ryu, B., Ahn, G., Yeo, I.-K., Jeon, Y.-J., 2020. Therapeutic potential of algal natural products against metabolic syndrome: a review of recent developments. Trends Food Sci. Technol. 97, 286–299. https://doi.org/10.1016/j.tifs.2020.01.020.

Fiorito, S., Genovese, S., Epifano, F., Mathieu, V., Kiss, R., Taddeo, V.A., 2016. Cytotoxic activity of lomatiol and 7-(3 '-Hydroxymethy1-3 '-methylallyloxy)coumarin. Nat Prod Commun 11, 407–408.

Fiorito, S., Preziuso, F., Epifano, F., Scotti, L., Bucciarelli, T., Taddeo, V.A., Genovese, S., 2019. Novel biologically active principles from spinach, goji and quinoa. Food Chem. 276, 262–265. https://doi.org/10.1016/j.foodchem.2018.10.018.

FitzGerald, R.J., Cermeño, M., Khalesi, M., Kleekayai, T., Amigo-Benavent, M., 2020. Application of in silico approaches for the generation of milk protein-derived bioactive peptides. J Funct Foods 64, 103636. https://doi.org/10.1016/j.jff.2019.103636.

Franco, R.R., Alves, V.H.M., Zabisky, L.F.R., Justino, A.B., Martins, M.M., Saraiva, A.L., Goulart, L.R., Espindola, F.S., 2020. Antidiabetic potential of Bauhinia forficata Link leaves: a non-cytotoxic source of lipase and glycoside hydrolases inhibitors and molecules with antioxidant and antiglycation properties. Biomed. Pharmacother. 123, 109798. https://doi.org/10.1016/j.biopha.2019.109798.

Gargaro, M., Epifano, F., Fiorito, S., Taddeo, V.A., Genovese, S., Pirro, M., Turco, A., Puccetti, P., Schmidt-Weber, C.B., Fallarino, F., 2017. Interaction of 7-alkoxycoumarins with the aryl hydrocarbon receptor. J. Nat. Prod. 80, 1939–1943. https://doi.org/10.1021/acs.jnatprod.7b00173.

Genovese, S., Epifano, F., Carlucci, G., Marcotullio, M., Curini, M., Locatelli, M., 2010. Quantification of 4′-geranyloxyferulic acid, a new natural colon cancer chemopreventive agent, by HPLC-DAD in grapefruit skin extract. J Pharmaceut Biomed 53, 212–214. https://doi.org/10.1016/j.jpba.2010.01.041.

Genovese, S., Epifano, F., Curini, M., Dudra-Jastrzebska, M., Luszczki, J.J., 2009. Prenyloxyphenylpropanoids as a novel class of anticonvulsive agents. Bioorg. Med. Chem. Lett 19, 5419–5422. https://doi.org/10.1016/j.bmcl.2009.07.110.

Genovese, S., Epifano, F., Fiorito, S., Curini, M., Marrelli, M., Menichini, F., Conforti, F., 2013. Conjugation of L-NAME to prenyloxycinnamic acids improves its inhibitory effects on nitric oxide production. Bioorg. Med. Chem. Lett 23, 2933–2935. https://doi.org/10.1016/j.bmcl.2013.03.050.

Genovese, S., Epifano, F., Fiorito, S., Taddeo, V.A., Preziuso, F., Fraternale, D., 2018. Modulation of the phenylpropanoid geranylation step in Anethum graveolens cultured calli by ferulic acid and umbelliferone. Ind. Crop. Prod. 117, 128–130. https://doi.org/10.1016/j.indcrop.2018.03.008.

Hargrove, J.L., Greenspan, P., Hartle, D.K., Dowd, C., 2011. Inhibition of aromatase and α-amylase by flavonoids and proanthocyanidins from Sorghum bicolor bran extracts. J. Med. Food 14, 799–807. https://doi.org/10.1089/jmf.2010.0143.

Hasan, F., Shah, A.A., Hameed, A., 2009. Methods for detection and characterization of lipases: a comprehensive review. Biotechnol. Adv. 27, 782–798. https://doi.org/10.1016/j.biotechadv.2009.06.001.

Herrera, T., del Hierro, J.N., Fornari, T., Reglero, G., Martin, D., 2019. Inhibitory effect of quinoa and fenugreek extracts on pancreatic lipase and α-amylase under in vitro traditional conditions or intestinal simulated conditions. Food Chem. 270, 509–517. https://doi.org/10.1016/j.foodchem.2018.07.145.

Kayukova, L.A., Uzakova, A.B., Baitursynova, G.P., Dyusembaeva, G.T., Shul'gau, Z.T., Gulyaev, A.E., Sergazy, S.D., 2019. Inhibition of α-amylase and α-glucosidase by new β-aminopropionamidoxime derivatives. Pharm. Chem. J. 53, 37–41. https://doi.org/10.1007/s11094-019-01966-5.

Krissinel, E., Henrick, K., 2007. Inference of macromolecular assemblies from crystalline state. J. Mol. Biol. 372, 774–797. https://doi.org/10.1016/j.jmb.2007.05.022.

Li, C., Begum, A., Numao, S., Park, K.H., Withers, S.G., Brayer, G.D., 2005. Acarbose rearrangement mechanism implied by the kinetic and structural analysis of human pancreatic α-amylase in complex with analogues and their elongated counterparts. Biochemistry 44, 3347–3357. https://doi.org/10.1021/bi048334e.

Miners, J.O., Smith, P.A., Sorich, M.J., McKinnon, R.A., Mackenzie, P.I., 2004. Predicting human drug glucuronidation parameters: application of in vitro and in silico modeling approaches. Annu. Rev. Pharmacol. Toxicol. 44, 1–25. https://doi.org/10.1146/annurev.pharmtox.44.101802.121546.

Miyazaki, T., Shirakami, Y., Mizutani, T., Maruta, A., Ideta, T., Kubota, M., Sakai, H., Ibuka, T., Genovese, S., Fiorito, S., Taddeo, V.A., Epifano, F., Tanaka, T., Shimizu, M., 2021. Novel FXR agonist nelumal A suppresses colitis and inflammation-related colorectal carcinogenesis. Sci Rep-Uk 11. https://doi.org/10.1038/s41598-020-79916-5.

Nagy, N., Kuipers, H.F., Frymoyer, A.R., Ishak, H.D., Bollyky, J.B., Wight, T.N., Bollyky, P.L., 2015. 4-Methylumbe liferone treatment and hyaluronan innibition as a therapeutic strategy in nflammation, autoimmunity, and cancer. Front. Immunol. 6 https://doi.org/10.3389/fimmu.2015.00123.

Patil, M., Patil, R., Bhadane, B., Mohammad, S., Maheshwari, V., 2017. Pancreatic lipase inhibitory activity of phenolic inhibitor from endophytic Diaporthe arengae. Biocatal Agric Biotechnol 10, 234–238. https://doi.org/10.1016/j.bcab.2017.03.013.

Preziuso, F., Genovese, S., Marchetti, L., Sharifi-Rad, M., Palumbo, L., Epifano, F., Fiorito, S., 2020. 7-Isopentenyloxycoumarin: what is new across the last decade. Molecules 25. https://doi.org/10.3390/molecules25245923. ARTN 5923.

Ren, L., Qin, X., Cao, X., Wang, L., Bai, F., Bai, G., Shen, Y., 2011. Structural insight into substrate specificity of human intestinal maltase-glucoamylase. Protein Cell 2, 827–836. https://doi.org/10.1007/s13238-011-1105-3.

Spínola, V., Llorent-Martínez, E.J., Castilho, P.C., 2020. Inhibition of α-amylase, α-glucosidase and pancreatic lipase by phenolic compounds of Rumex maderensis (Madeira sorrel). Influence of simulated gastrointestinal digestion on hyperglycaemia-related damage linked with aldose reductase activity and protein glycation. LWT 118, 108727. https://doi.org/10.1016/j.lwt.2019.108727.

Subbaramaiah, K., Howe, L.R., Bhardwaj, P., Du, B., Gravaghi, C., Yantiss, R.K., Zhou, X. K., Blaho, V.A., Hla, T., Yang, P., 2011. Obesity is associated with inflammation and elevated aromatase expression in the mouse mammary gland. Canc. Prev. Res. 4, 329–346. https://doi.org/10.1158/1940-6207.CAPR-10-0381.

Trott, O., Olson, A.J., 2010. AutoDock Vina: improving the speed and accuracy of docking with a new scoring function, efficient optimization, and multithreading. J. Comput. Chem. 31, 455–461. https://doi.org/10.1002/jcc.21334.

Wong, S.K., Chin, K.-Y., Suhaimi, F.H., Fairus, A., Ima-Nirwana, S., 2016. Animal models of metabolic syndrome: a review. Nutrition 13, 65. https://doi.org/10.1186/s12986-016-0123-9.

Zengin, G., Locatelli, M., Carradori, S., Mocan, A.M., Aktumsek, A., 2016. Total phenolics, flavonoids, condensed tannins content of eight Centaurea species and their broad inhibitory activities against cholinesterase, tyrosinase, α-amylase and α-glucosidase. Not Bot Horti Agrobo 44, 195–200. https://doi.org/10.15835/nbha44110259.